Available online at www.sciencedirect.com
SCIENCE DIRECT
Tetrahedron 62 (2006) 8550–8558
Tetrahedron

New dioxadiaza-, trioxadiaza- and hexaaza-macrocycles containing dibenzofuran units

Feng Li,[a] Rita Delgado,[a,b,*] Ana Coelho,[a,c] Michael G. B. Drew[d] and Vítor Félix[e]

[a]*Instituto de Tecnologia Química e Biológica, Chemistry Division, UNL, Apartado 127, 2781-901 Oeiras, Portugal*
[b]*Instituto Superior Técnico, Av. Rovisco Pais, 1049-001 Lisboa, Portugal*
[c]*Universidade de Évora, Departamento de Química, 7000 Évora, Portugal*
[d]*School of Chemistry, University of Reading, Whiteknights, Reading, RG6 6AD, UK*
[e]*Departamento de Química, CICECO, Universidade de Aveiro, 3810-193 Aveiro, Portugal*

Received 8 May 2006; accepted 21 June 2006
Available online 20 July 2006

Abstract—New dioxadiaza-, trioxadiaza-, and hexaaza-macrocycles containing rigid dibenzofuran groups (DBF) were prepared by a convenient synthetic route in high yields. The structures of the macrocycles were unequivocally established by electrospray mass spectrometry (ESIMS) studies together with NMR spectroscopy, with the exception of [14](DBF)N_3. The structures of the copper complex of [14](DBF)N_3 and of the diprotonated form of [22](DBF)N_2O_3 were determined by single crystal X-ray diffraction. Conformational analyses on the free macrocycles [14](DBF)N_3 and [22](DBF)N_2O_3 as well as on their larger counterparts containing two DBF units were undertaken in order to understand the synthetic findings.

1. Introduction

In recent years there have been an increasing interest in the design, synthesis and use of diverse macrocyclic receptors capable of selective recognition of metal ions, anions and neutral molecules,[1–4] since their cavity sizes, shapes and components can be readily modified. These features have led to the development of many applications, from catalysis to mediated transport, from sensors or devices and to molecular machines or pharmacology.[1–6]

We are interested in developing simple synthetic methods to prepare polyaza- or polyoxapolyaza-macrocyclic compound having rigid 4,6-dibenzofuran (DBF) units and flexible spacers able to recognize metal ions or organic substrates. The DBF group is not a common building block, nevertheless it has already been used to prepare supramolecular compounds or devices as a spacer in rigid macrocycles,[7,8] catenanes,[8] cavitands,[9,10] calixarenes[11] and rigidly preorganised clefts or as the central part of tweezers.[9,10,12–19] Most of the known compounds contain the 2,8- or 3,7-substituted DBF fragments.

In the present work, five novel polyaza- or polyoxadiaza-macrocycles incorporating the DBF structural fragments, [17](DBF)N_2O_2, [22](DBF)N_2O_3, [14](DBF)N_3, [28](DBF)$_2N_6$ and [32](DBF)$_2N_6$ (see Scheme 1), were synthesized by a [1+1] or [2+2] condensation of different linear amines with 4,6-dibenzofurandicarbaldehyde. All the prepared macrocycles display an important structural feature

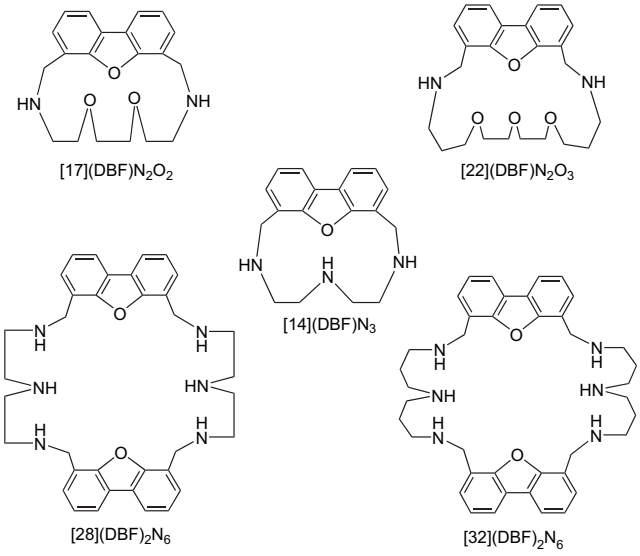

Scheme 1.

Keywords: Macrocycles; Dibenzofuran derivatives; X-ray structures; [2+2] Condensation.
* Corresponding author. Tel.: +351 214469737/8; fax: +351 215511277; e-mail: delgado@itqb.unl.pt

0040–4020/$ - see front matter © 2006 Elsevier Ltd. All rights reserved.
doi:10.1016/j.tet.2006.06.073

one or two rigid DBF moieties coupled at the 4 and 6 positions with flexible polyoxadiaza or polyaza spacers. The largest macrocycles, [22](DBF)N_2O_3, [28](DBF)$_2N_6$ and [32](DBF)$_2N_6$, are capable of coordinating one or two metal ions, while the smallest ones [14](DBF)N_3 and [17](DBF)N_2O_2 can only form mononuclear metal complexes. On the other hand, the hexaprotonated forms of [28](DBF)$_2N_6$ and [32](DBF)$_2N_6$ as well as their dimetal complexes are receptors for dianion substrates leading to the formation of stable supermolecules. The binding studies will be provided in future publications.

2. Results and discussion

2.1. Synthesis

The compounds [17](DBF)N_2O_2 and [22](DBF)N_2O_3 were prepared by the [1+1] cyclocondensation of 4,6-dibenzofurandicarbaldehyde with the appropriate diamine, 2,2′-ethylenedioxy-bis(ethylamine) and 4,7,10-trioxa-1,13-tridecanediamine, respectively, while [28](DBF)$_2N_6$ and [32](DBF)$_2N_6$ resulted from the [2+2] cyclocondensation with diethylenetriamine and *N*-(3-aminopropyl)-1,3-propanediamine, respectively. In all cases low temperature was used and the desired macrocycles were obtained in high yield after reduction of the corresponding Schiff bases with $NaBH_4$ (see Scheme 2). Several attempts to obtain the larger macrocycles [34](DBF)$_2N_4O_4$ and [44](DBF)$_2N_4O_6$ via [2+2] condensation using the corresponding polyoxadiamine were undertaken without success, in spite of the use of experimental conditions favouring thermodynamically the formation of these larger molecules, low temperature and high dilution. The resulting products ([1+1] or [2+2]) were distinguished by mass spectrometry.

The macrocycles [17](DBF)N_2O_2 and [22](DBF)N_2O_3 were isolated as white powders from ethanolic hydrobromic acid solutions, while pure [28](DBF)$_2N_6$ and [32](DBF)$_2N_6$ were obtained by recrystallization of the crude product from ethanol. The macrocycle [14](DBF)N_3 found in a small amount, as a side-product of the synthesis of [28](DBF)$_2N_6$, was isolated from the liquor mother ethanol solutions as a copper(II) complex by addition of $CuSO_4$. The X-ray single crystal structure of this complex was determined showing definitely that the [1+1] product was also formed, see below. Then the synthesis of [14](DBF)N_3 as a single product was attempted in conditions favouring the [1+1]

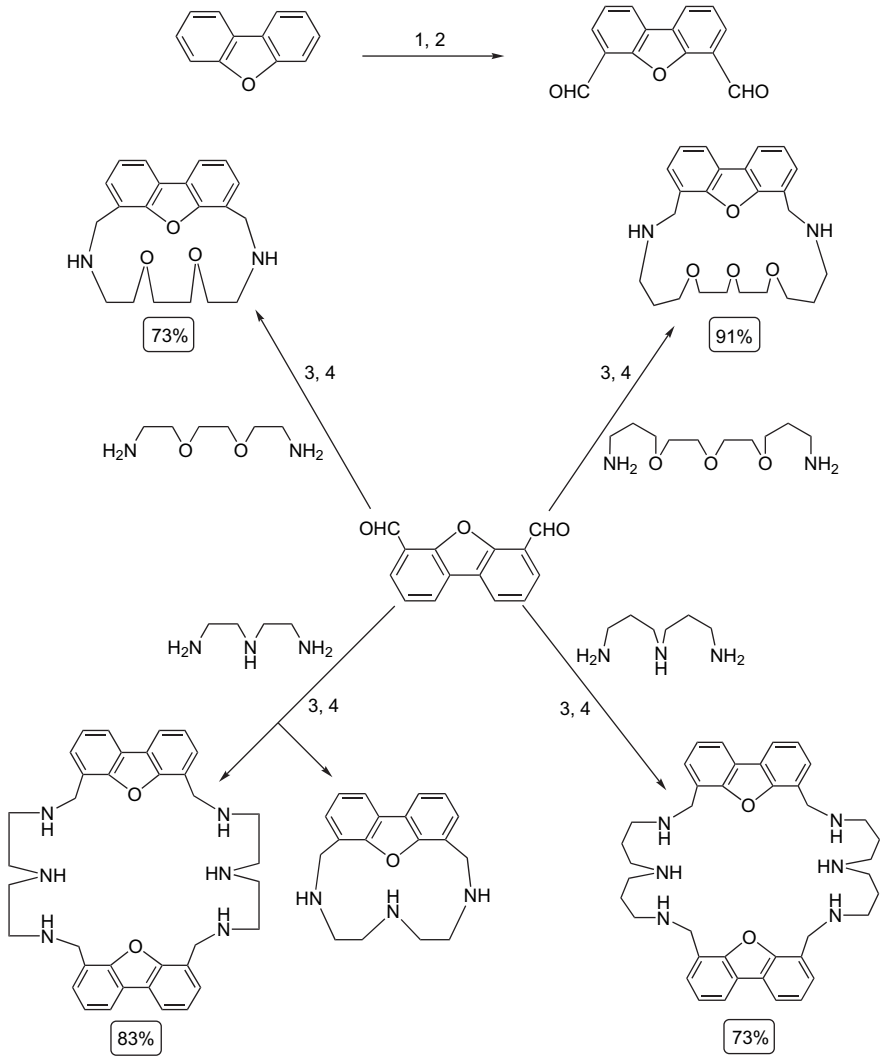

Scheme 2. (1) Et_2O, TMEDA, *n*-BuLi, reflux; (2) DMF, 0 °C, then rt 24 h; (3) EtOH, 0 °C and (4) $NaBH_4$, rt.

product, but surprisingly in spite of our best efforts all the synthetic routes always yielded the larger macrocycle as the main product.

Condensation of 4,6-dibenzofurandicarbaldehyde with the aromatic spacer *m*-xylylenediamine or different aliphatic polyamines having longer chains, such as 3,3′-ethylenediiminodipropylamine and triethylenetetramine, was also carried out in the experimental conditions described above. However the work-up of these syntheses revealed the presence of mixtures of polymers and other macrocycles and the isolation of the expected macrocycles was impossible.

The dioxadiamine and trioxadiamine mainly yielded to [1+1] cyclocondensation products while both triamines seem to favour the formation of larger macrocycles via [2+2] condensation. This synthetic finding led us to think that intramolecular bonding interactions, such as hydrogen bonds, play a role in the preorganization of different intermediate compounds involved in the final stage of cyclocondensation process determining the synthetic route followed (we recall to this point bellow).

Other approaches involving one-pot reaction for the synthesis of similar macrocycles require a template or high dilution. However, these synthetic routes yield in general to complicated work-up, more difficult product purifications, and waste of solvents.[20–22]

2.2. Electrospray mass spectrometry studies

The ESI mass spectra acquired in positive polarity mode using methanol solutions of [17](DBF)N_2O_2, [22](DBF)N_2O_3, [28](DBF)$_2N_6$ and [32](DBF)$_2N_6$ showed peaks corresponding to the monoprotonated ligands. In the spectra of [17](DBF)N_2O_2 and [28](DBF)$_2N_6$ *m*/*z* peaks (363.3 and 613.1, respectively) corresponding to the sodium adducts of the macrocycles are present. A low intensity *m*/*z* peak at 296.0 was also observed in the [28](DBF)$_2N_6$ mass spectrum that can be assigned to the $[M+2H]^{2+}$ diprotonated form. The intensity of this peak was increased when 0.1% formic acid was added to the macrocycle dissolved in methanol. The spectrum of [32](DBF)$_2N_6$ also contains one weak peak corresponding to the double protonated ion $[M+2H]^{2+}$ (*m*/*z* 324).

2.3. X-ray crystallographic studies

In the X-ray crystal structure discrete units of $\{H_2[22](DBF)N_2O_3\}^{2+}$ and two independent PF_6^- anions are held together by hydrogen-bonding interactions between the fluoride atoms and the two N–H binding sites leading to the formation of the supermolecule as shown in Figure 1. The dimensions of all hydrogen-bonding interactions found are listed in Table 1. Both PF_6^- anions are located outside of the macrocyclic cavity. The first PF_6^- anion is involved in only one N···H–F hydrogen bond with a N···F distance of 2.18 Å, while the second one is involved in a bifurcated

Table 1. Dimensions of the hydrogen bonds of **1** and **2**

Donor–H···acceptor	H···A/Å	D···A/Å	D–H···A/°
$\{H_2[22](DBF)N_2O_3\}\cdot 2PF_6$ (**1**)			
Intermolecular			
N(16)–H(16A)···F(13)	2.18	2.926(2)	140
N(30)–H(30A)···F(21)	2.02	2.888(2)	161
N(30)–H(30A)···F(23)	2.34	3.059(2)	136
Intramolecular			
N(16)–H(16B)···O(20)	2.15	2.741(2)	123
N(16)–H(16B)···O(23)	2.02	2.863(2)	156
N(30)–H(30B)···O(26)	2.12	2.833(2)	136
N(16)–H(16A)···O(26)	2.44	3.044(2)	125
$[Cu([14](DBF)N_3)(H_2O)_2](SO_4)\cdot 3H_2O$ (**2**)			
N(16)–H(16)···O(500)	2.04	2.940(11)	170
N(19)–H(19)···O(21) [2-*x*,1-*y*,1-*z*]	2.31	3.120(10)	149
N(22)–H(22)···O(23)	2.58	3.177(10)	124
N(22)–H(22)···O(300) [2-*x*,1-*y*,1-*z*]	2.46	3.226(11)	142
O(100)–H(101)···O(300)	1.99(5)	2.745(11)	155(4)
O(100)–H(102)···O(22)	2.15(6)	2.743(10)	130(6)
O(200)–H(201)···O(24) [2-*x*,2-*y*,1-*z*]	1.98(4)	2.681(8)	146(4)
O(200)–H(202)···O(23)	1.95(4)	2.718(10)	159(5)
O(300)–H(301)···O(500)	2.24(7)	2.885(12)	136(7)
O(300)–H(302)···O(21) [2-*x*,1-*y*,1-*z*]	1.99(8)	2.765(10)	159(8)
O(400)–H(401)···O(23)	2.09(6)	2.890(10)	167(10)
O(400)–H(402)···O(22) [2-*x*,2-*y*,1-*z*]	2.19(9)	2.976(11)	161(11)
O(500)–H(501)···O(400) [2-*x*,2-*y*,1-*z*]	2.04(8)	2.817(13)	158(8)

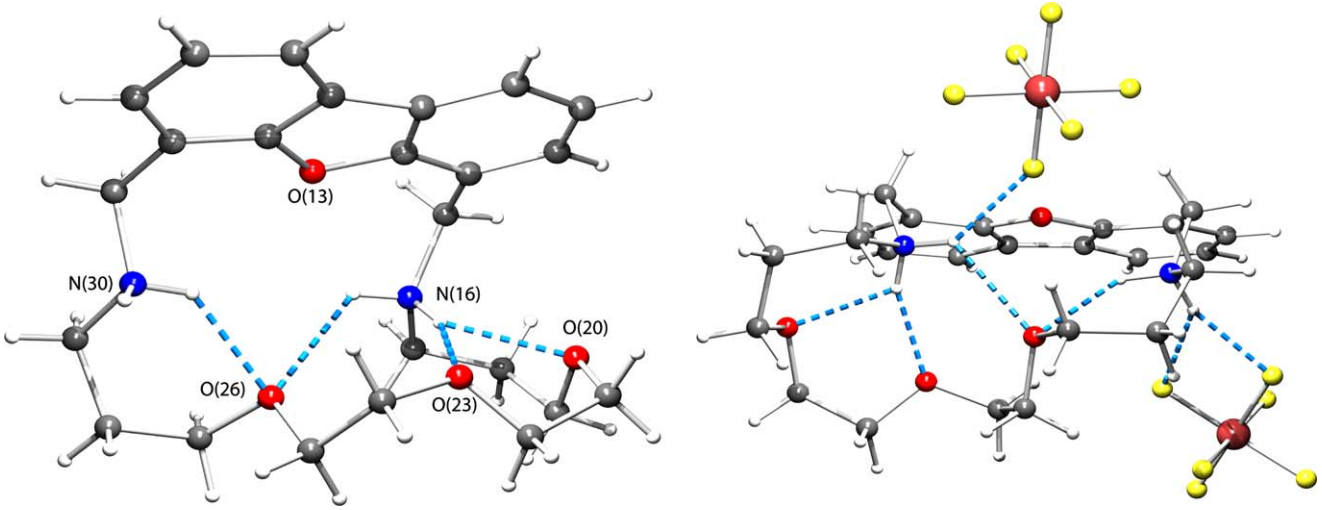

Figure 1. Structure of the supramolecular association found in solid state for $\{H_2[22](DBF)N_2O_3\}\cdot 2PF_6$. Molecular structure of $\{H_2[22](DBF)N_2O_3\}^{2+}$ with the labelling scheme adopted (left) and the supramolecular interaction between $\{H_2[22](DBF)N_2O_3\}^{2+}$ and PF_6^- anion (right).

hydrogen-bonding interaction with a N–H binding site of the second nitrogen donor atom, the H···F distances being 2.02 and 2.34 Å. Three N–H binding sites are directed toward the electron lone pairs of three oxygen donors leading to the formation of four intramolecular N–H···O hydrogen bonds with H···O distances of 2.02, 2.12, 2.15 and 2.44 Å. These hydrogen-bonding interactions are certainly important for the stabilization of the conformation presented in Figure 1 (left) for the protonated receptor.

The X-ray single crystal diffraction of the Cu(II) complex with [14](DBF)N_3 is built up from an asymmetric unit composed of one $[Cu([14](DBF)N_3)(H_2O)_2]^{2+}$ cation (1), one SO_4^{2-} as the counter-ion and three water molecules. The molecular structure of $[Cu([14](DBF)N_3)(H_2O)_2]^{2+}$ with the labelling scheme adopted is presented in Figure 2. The copper atom shows a distorted octahedral coordination environment with the equatorial plane determined by the three nitrogen donor atoms with Cu–N distances ranging from 2.106(7) to 2.138(7) Å and an oxygen atom from a water molecule with a Cu–O of 2.037(6) Å. The axial positions are occupied by oxygen atoms from the DBF moiety and of the second coordination water molecule at Cu–O distances of 2.059(6) and 2.352(5) Å, respectively. The copper centre is 0.110(3) Å away from the equatorial coordination plane towards the apical water molecule. This geometric arrangement is achieved with the folding of the macrocycle along the N(22)–N(16) axis leading to a dihedral angle between the DBF moiety and the plane defined by the three nitrogen donor atoms of 75.8(3)°. Selected bond length angles subtended at the copper centre are given in Table 2. The longest Cu–O apical distance reveals a tetragonal distortion, which is expected for metal complexes with d^9 electronic configuration. The Cu–N distances found are within the typical values reported for azamacrocylic complexes with copper bonded to N_{sp^3} nitrogen donor.[23]

In the crystal structure the ionic species $[Cu([14](DBF)N_3)(H_2O)_2]^{2+}$ and SO_4^{2-}, and water solvent molecules are assembled by an extensive 1-D chain of hydrogen bonds along the [010] base vector as shown in Figure 2 (right). Their molecular dimensions are listed in Table 1 together with those found for $\{H_2[22](DBF)N_2O_3\}\cdot 2PF_6$. The SO_4^{2-} anions link directly three adjacent $[Cu([14](DBF)N_3)(H_2O)_2]^{2+}$ cations through the five independent hydrogen bonds with two N–H groups (H···O= 2.31 and 2.58 Å), two with equatorial coordinated water molecule (H···O=1.98(4) and 1.95(4) Å) and one with axial coordinated water (H···O=2.15(6) Å). This pattern of hydrogen bonds leads to the formation of 1-D network, which is completed by multiple hydrogen bonds between water bridges composed of three water molecules with the third N–H binding site (H···O=2.04 Å), axial coordinated water molecule (H···O=1.99(5) Å) and SO_4^{2-} anions with H···O distances ranging from 1.99(8) to 2.19(9) Å. The O···H distances within the water bridge are 2.04(8) and 2.24(7) Å.

Table 2. Selected bond lengths (Å) and angles (°) for $[Cu([14](DBF)N_3)(H_2O)_2]^{2+}$

Cu–O(13)	2.352(5)	Cu–O(100)	2.059(6)
Cu–O(200)	2.037(6)	Cu–N(16)	2.106(7)
Cu–N(19)	2.123(7)	Cu–N(22)	2.138(7)
N(16)–Cu–N(22)	160.6(2)		
O(100)–Cu–O(13)	172.9(2)	O(200)–Cu–N(19)	174.6(3)
O(200)–Cu–O(100)	92.0(2)	O(200)–Cu–N(16)	100.4(2)
O(100)–Cu–N(16)	101.8(3)	O(100)–Cu–N(19)	92.0(3)
N(16)–Cu–N(19)	82.5(3)	O(200)–Cu–N(22)	93.7(3)
O(100)–Cu–N(22)	91.0(3)	N(19)–Cu–N(22)	82.5(3)
O(200)–Cu–O(13)	84.7(2)	N(16)–Cu–O(13)	85.0(2)
N(19)–Cu–O(13)	91.0(2)	N(22)–Cu–O(13)	83.0(2)

To the best of our knowledge, the two structures reported here represent the first two examples of oxaazamacrocycles incorporating DBF moieties in their skeletons. Indeed a search on Cambridge Data Base[24] retrieved only 11 crystal structures of macrocyclic compounds with BDF moieties. In seven of them, the BDF fragment is bridging two porphyrin platforms used to anchor two metal transition centres (refcodes ATIREA, INUWOD, LIRSEK, LIRSIO

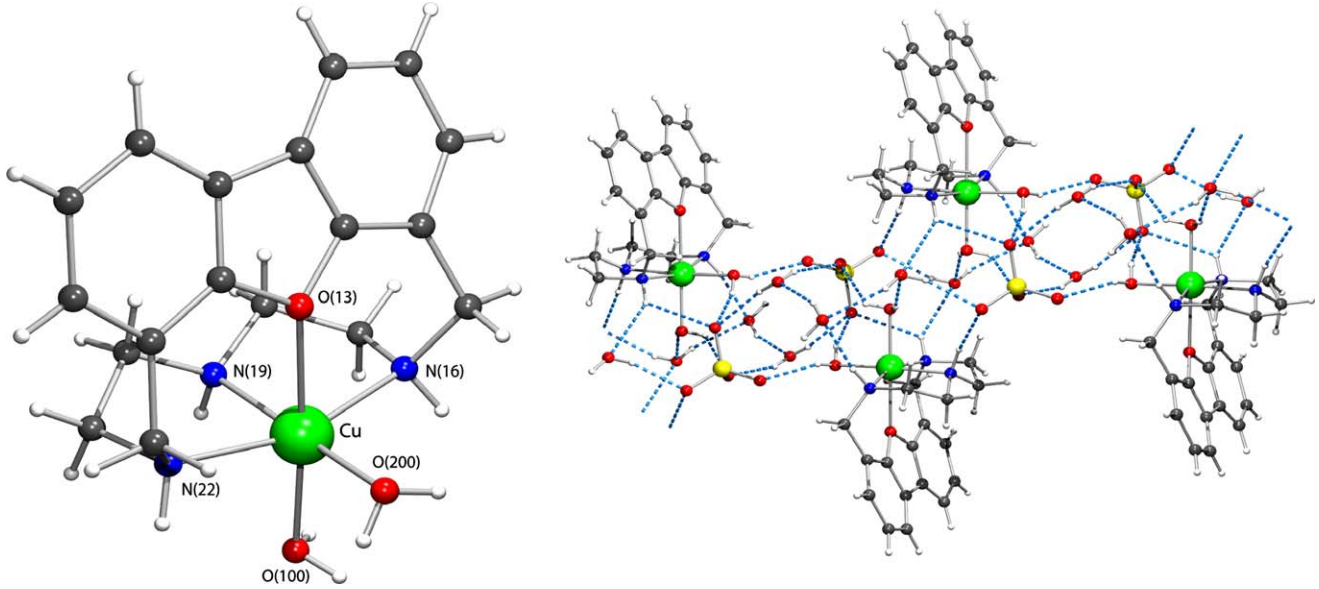

Figure 2. X-ray single crystal structure of $[Cu([14](DBF)N_3)(H_2O)_2](SO_4)\cdot 3H_2O$. Molecular structure of $[Cu([14](DBF)N_3)(H_2O)_2]^{2+}$ with the labelling scheme adopted (left) and crystal packing diagram showing the 1-D network of N–H···O hydrogen bonds (right).

and LOMLAA) or not (refcodes MOBVOO and OFOSIL). In the remaining four compounds, the macrocycle incorporates one (refcode AFILUW), three (refcodes JUSXOK and JUSYAX) or four (JUSXIE) coupled DBF structural units. The compound, with the refcode JUSYAX is the unique azamacrocycle and displays a rigid structure with three-DBF units head connected by a small dimethyl-ethylenodiamine spacer.

2.4. Molecular modelling

In order to give a further insight on the influence of structural features in the cyclocondensation process, i.e., the formation of smaller or larger macrocycles, conformational analyses were undertaken for [14](DBF)N_3 and [22](DBF)N_2O_3 and their larger counterpart ones [28](DBF)$_2N_6$ and [44](DBF)$_2N_4O_6$ via molecular dynamics quenching methods using AMBER-8 software package.[25] Atomic parameters were taken from the GAFF force field[26] and the atomic partial charges for neutral species were calculated with the AM1-BCC method.[27] The structures of all four macrocycles were heated in the gas phase at 2000 K for 1 ns using a time step of 1 fs. Snapshots were saved for every 0.1 ps leading to trajectory files containing 10 000 frames, which were subsequently energy-minimized using an appropriate house script.

For [14](DBF)N_3 the lowest energy structure was found at 78.9 kcal mol^{-1} and displays a folded conformation with the DBF unit making with the plane of the nitrogen donors a dihedral angle of 71.9°. The two N–H groups adjacent to DBF unit are at a short O···H distances of 2.31 Å from the oxygen donor leading to two N–H···O hydrogen bonds with angles 131°. Furthermore, both N–H groups also form N–H···N hydrogen bonds with the N–H group opposite to DBF unit having a N···H distances of 2.16 Å and the N–H···N angles of 117°. Thus, the simultaneous occurrence of four intramolecular hydrogen-bonding contacts leads to a lowest energy conformation with an apparent rigid structure. The first roughly planar energy conformation is only 0.95 kcal mol^{-1} above the minimum energy conformation. The N–H group opposite to the oxygen donor is involved with it in a strong hydrogen-bonding with a H···O distance of 2.19° and N–H···O angle of 175°.

The first three conformations of [28](DBF)$_2N_6$ with energy ranging between 145.1 and 147.1 kcal mol^{-1} exhibit the aromatic DBF unit in an almost parallel arrangement, as shown in Figure 3, which suggests the presence of a π–π bonding interaction. Furthermore, all three conformations show at least a single hydrogen bond interaction involving a N–H group and an oxygen donor from the DBF unit. For example, the lowest energy conformation exhibits a N–H group pointing to the oxygen from a DBF unit at H···O distance of 2.37 Å giving a N–H···O angle of 129°. In addition, this conformation reveals four N–H···N hydrogen-bonding interactions. Three of them are hydrogen bonds between neighbour N–H groups with H···N distances ranging from 2.41 to 2.57 Å. The remaining one with a H···N distance of 2.01 Å and a N–H···N angle of 160° is the most strong and occurs between two N–H groups from different spacers suggesting that they play an important role in the stabilization of the lowest energy conformation. It is interesting to note that short N–H···N hydrogen-bonding contacts are also present in the next lowest energy conformations.

The lowest five energy conformations found for [22](DBF)N_2O_3 have energies between 42.3 and 44.9 kcal mol^{-1} with the DBF unit tilted relatively to the N_2O_3 plane and all display two hydrogen bonds. In three of them, the N–H···O intramolecular bonding contacts with H···O distances ranging from 2.07 to 2.36 Å occur only between N–H groups and ether oxygen donors of the spacer as observed in the crystal structure of $\{H_2[22](DBF)N_2O_3\}^{2+}$ (see above). The fourth conformation has an energy of 44.1 kcal mol^{-1} and the hydrogen bonds involve the oxygen donors from the spacer and the DBF unit with H···O distances of 1.96 and 2.30 Å, respectively. These conformational types are illustrated in Figure 4, which shows the lowest energy structures of [22](DBF)N_2O_3 and [44](DBF)$_2N_4O_6$. As would be expected the largest macrocycle [44](DBF)$_2N_4O_6$ has enough flexibility to adopt very different conformations with similar energies. Indeed the two lowest energy conformations have different arrangements of the two DBF units. In the first, these units have an almost perpendicular spatial disposition, while in the second they are almost parallel making dihedral angles of ca. 90° and 0°, respectively. As a consequence of the perpendicular orientation of two units in the first conformation, one C–H hydrogen from one DBF unit is directed towards the aromatic ring of the second one at a distance of 2.58 Å, which suggests the presence of edge to face C–H(σ)···π interaction. The dimensions of this macrocycle also allow the establishment of isolated hydrogen bonds without any apparent steric strain, as happens in the second lowest energy conformation, which has a short H···O contact of 2.40 Å. Both polyoxapolyaza-macrocycles, [22](DBF)N_2O_3 and [44](DBF)$_2N_4O_6$, do not show N–H···N hydrogen-bonding interactions in

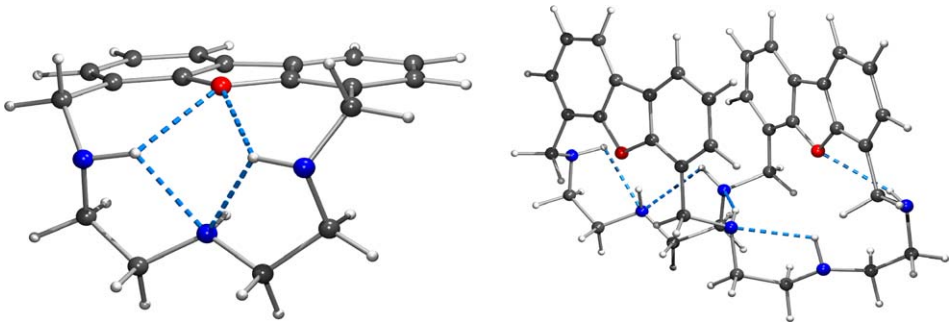

Figure 3. Structures of the lowest energy conformations found with GAFF force field[26] for [14](DBF)N_3 (left) and [28](DBF)$_2N_6$ (right).

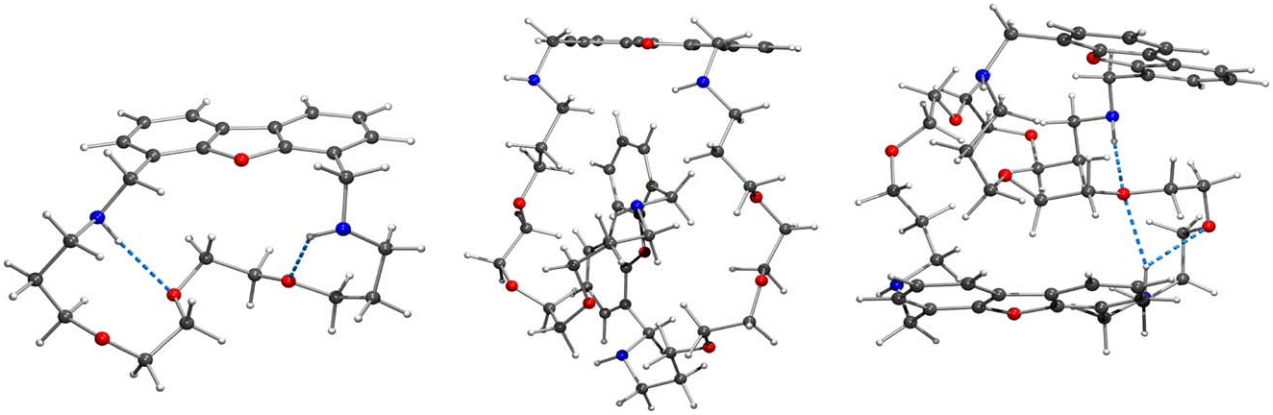

Figure 4. Lowest energy conformations for [22](DBF)N_2O_3 (left) and [44](DBF)$_2N_4O_6$ (centre and right).

all the low energy minimized structures found by conformational analyses, which is in contrast with what was observed for the two polyaza-macrocycles, [14](DBF)N_3 and [28](DBF)$_2N_6$.

2.5. Conclusions

A new series of polyoxapolyaza- or polyaza-macrocyclic receptors containing 4,6-dibenzofuran units was prepared in high yield with a convenient synthetic route, which did not require high dilution or template techniques. The electrospray ionization mass spectrometry ESIMS technique was successfully used for preliminary analysis and determination of the stoichiometry of the macrocyclic compounds. The X-ray single crystal structure of the copper complex with [14](DBF)N_3 confirmed that the [1+1] condensation of 4,6-dibenzofurandicarbaldehyde with diethylenetriamine also occurred.

It is interesting to note that the condensation of 4,6-dibenzofurandicarbaldehyde with different diamines, at the same reaction conditions, led preferentially to [1+1] macrocycles in certain cases and to [2+2] in others. Indeed the dioxa- and trioxa-diamines used to undergo [1+1] condensations while both triamines led to [2+2] ones. The crystal structure of the protonated [22](DBF)N_2O_3 macrocycle displays three intramolecular N–H···O hydrogen-bonding interactions suggesting that the formation of the free macrocycle via [1+1] cyclocondensation can be favoured. In order to bring some light to this point the structural preferences of the macrocycles [14](DBF)N_3, [22](DBF)N_2O_3, [28](DBF)$_2N_6$ and [44](DBF)$_2N_4O_6$ were investigated through conformational analysis using the GAFF force field. The smaller macrocycles in their lowest energy structures have two N–H···O hydrogen bonds. In [14](DBF)N_3, these interactions are accomplished by two extra N–H···N hydrogen bonds leading to an apparent rigid structure. These facts suggest that intramolecular hydrogen-bonding interactions N–H···O and/or N–H···N can be present in the [1+1] cyclocondensation process, pre-organizing the corresponding intermediate in an almost rigid arrangement for the final cyclization step of the smaller macrocycles. Multiple N–H···N bonding interactions were observed in [28](DBF)$_2N_6$ suggesting that the formation of this larger macrocycle is favoured relatively to the smaller counterpart by the cooperative effect induced by this set of hydrogen bonds. In contrast, this type of interaction was not observed for the polyoxapolyaza-macrocycles, [22](DBF)N_2O_3 and [44](DBF)$_2N_4O_6$, and only the first one was obtained. Furthermore, the theoretical calculations also indicated that in the gas phase, other factors can contribute to the final cyclization product, as happens with [28](DBF)$_2N_6$, in which the intramolecular arrangement suggests the presence of π–π stacking interactions. Of course, the molecular modelling studies described here are somewhat simplistic as only the structural features were considered, relegating other factors certainly important for the formation of these macrocycles, such as solvation and entropy changes. Studies of the metal coordination and supramolecular properties of these novel polyaza- and polyoxapolyaza-macrocycles are in progress in our laboratories.

3. Experimental

3.1. Reagents

The compounds 4,6-dibenzofuran, 2,2′-ethylenedioxy-bis-(ethylamine), 4,7,10-trioxa-1,13-tridecanediamine, diethylenetriamine and *N*-(3-aminopropyl)-1,3-propanediamine were obtained from a commercial supplier and used as received unless noted , 4,6-dibenzofurandicarbaldehyde was prepared by reported method.[28] For mass spectra acquisition LC–MS grade solvents were used. The reference used for the ^{1}H NMR measurements in D_2O was the 3-(trimethylsilyl)-propanoic acid-d_4-sodium salt and in $CDCl_3$ the solvent itself (at 7.26 ppm). For ^{13}C NMR spectra in D_2O, 1,4-dioxane (signal at 67.15 ppm) was used as an internal reference.

3.2. Synthesis of [17](DBF)N_2O_2

The 4,6-dibenzofurandicarbaldehyde (0.5 g, 2.23 mmol) was suspended in ethanol (150 cm^3) and the mixture left stirring in an ice-bath for half an hour. To this solution, 2,2′-ethylenedioxy-bis(ethylamine) (0.33 g, 2.23 mmol) in ethanol (50 cm^3) was added dropwise during 3–4 h, and left stirring for overnight at 0 °C. The 4,6-dibenzofurandicarbaldehyde dissolved in the ethanol solution during the reaction. At the end the yellow solution became completely transparent. Then $NaBH_4$ (0.7 g, 18.5 mmol) was directly added into the same reactor and the solution was left overnight at room temperature. Ethanol was removed and the remaining grey product was dissolved in water (50 cm^3).

The pH of the aqueous solution was increased to 12 with NaOH and extraction with chloroform (5×30 cm^3) was carried out. The organic phases were combined, dried with Na_2SO_4 and completely evaporated under *vacuum* to obtain a yellow oil. This oil was dissolved in ethanol (30 cm^3) and 48% hydrobromic acid (about 2 cm^3). The desired product was precipitated in the form of a white HBr-salt. Yield: 73.7%, mp 261–262 °C (dec). ^{1}H NMR (D_2O): δ 3.35 (br s, 4H), 3.71 (br s, 4H), 3.83 (s, 4H), 4.54 (s, 4H), 7.42 (t, J=7.4 Hz, 2H), 7.50 (d, J=7.1 Hz, 2H) and 8.09 (d, J=7.4 Hz, 2H). ^{13}C NMR (D_2O): δ 48.1, 49.2, 67.5, 72.4, 117.2, 125.4, 126.6, 126.7, 132.0 and 156.4. Found: C, 47.87; H, 5.52; N, 5.65%. Calcd for $C_{20}H_{24}N_2O_3\cdot2HBr$: C, 47.83; H, 5.22; N, 5.58%. IR (KBr pellets, cm^{-1}): 3428, 2934, 2794, 1437, 1422, 1189, 1130, 1104, 785, 746. ESIMS, *m*/*z* 341.2 [M+H]$^+$.

3.3. Synthesis of [22](DBF)N_2O_3

A similar procedure to the one described above was employed to prepare [22](DBF)N_2O_3 from 4,6-dibenzofurandicarbaldehyde (0.5 g, 2.23 mmol) and 4,7,10-trioxa-1,13-tridecanediamine (0.49 g, 2.23 mmol). After extraction the organic phases were combined, dried with Na_2SO_4 and completely evaporated under *vacuum* to obtain the yellow oil. This oil was dissolved in ethanol (30 cm^3), and 48% hydrobromic acid (about 2 cm^3) was added. The desired product was precipitated in the form of a white HBr-salt. Yield: 91.4%, mp 281–282 °C (dec). ^{1}H NMR (D_2O): δ 1.97 (t, J=5.9 Hz, 4H), 3.26 (t, J=7.1 Hz, 4H), 3.58 (m, 12H), 4.50 (s, 4H), 7.40 (t, J=7.5 Hz, 2H), 7.48 (d, J=7.5 Hz, 2H) and 8.05 (d, J=7.5 Hz, 2H). ^{13}C NMR (D_2O): δ 27.8, 47.7, 48.1, 70.5, 71.8, 71.9, 117.1, 125.5, 126.6, 126.7, 131.9 and 156.5. Found: C, 50.43; H, 6.42; N, 5.03%. Calcd for $C_{24}H_{32}N_2O_4\cdot2HBr$: C, 50.19; H, 5.97; N, 4.88%. IR (KBr pellets, cm^{-1}): 3437, 2950, 2798, 1437, 1425, 1201, 1109, 845, 781, 748. ESIMS, *m*/*z* 413.0 [M+H]$^+$.

3.4. Synthesis of [28](DBF)$_2N_6$ and of the complex [Cu([14](DBF)N_3)(H_2O)$_2$](SO_4)$^{2-}\cdot3H_2O$

A similar procedure to the one described above was employed to prepare [28](DBF)$_2N_6$ from 4,6-dibenzofurandicarbaldehyde (0.5, 2.23 mmol) and diethylenetriamine (0.23 g, 2.23 mmol). After evaporation of the solvent from extraction, the recrystallization of the residue from ethanol provided 0.55 g (83.4%) of [28](DBF)$_2N_6$ as a white solid. Mp 187–189 °C (dec). ^{1}H NMR ($CDCl_3$): δ 1.90 (br s, 6H), 2.76 (s, 16H), 4.14 (s, 8H), 7.25 (t, J=7.5 Hz, 4H), 7.32 (d, J=6.9 Hz, 4H) and 7.82 (d, J=7.5 Hz, 4H). ^{13}C NMR ($CDCl_3$): δ 48.6, 48.8, 49.2, 119.5, 122.8, 124.2, 124.3, 127.3 and 154.5. Found: C, 73.0; H, 7.18; N, 14.17%. Calcd for $C_{36}H_{42}N_6O_2$: C, 73.19; H, 7.17; N, 14.23%. IR (KBr pellets, cm^{-1}): 3427, 3281, 2922, 2833, 1432, 1185, 845, 770, 747. ESIMS, *m*/*z* 591.1 [M+H]$^+$.

An aqueous solution of $CuSO_4\cdot5H_2O$ (0.04 mmol, 0.01 g) was directly added to the ethanolic mother solution of [28](DBF)$_2N_6$ and the mixture was stirred for 1 h. The solvent was removed under *vacuum*. The solid was dissolved in a mixture of acetonitrile/methanol (1:1). Blue crystals were formed in two weeks by slow evaporation of the solvent at room temperature.

3.5. Synthesis of [32](DBF)$_2N_6$

A similar procedure to the one described above was employed to prepare [32](DBF)$_2N_6$ from 4,6-dibenzofurandicarbaldehyde (0.5 g, 2.23 mmol) and *N*-(3-aminopropyl)-1,3-propanediamine (0.30 g, 2.23 mmol). After evaporation of the solvent resulting from the extraction, the recrystallization of the residue from ethanol provided 0.53 g (73.4%) of [32](DBF)$_2N_6$ as a white solid. Mp 172–173 °C (dec). ^{1}H NMR ($CDCl_3$): δ 1.72 (t, J=6 Hz, 14H), 2.68 (t, J=6.9 Hz, 8H), 2.72 (t, J=6.9 Hz, 8H), 4.15 (s, 8H), 7.28 (t, J=7.5 Hz, 4H), 7.38 (d, J=6.9 Hz, 4H) and 7.82 (d, J=7.2 Hz, 4H). ^{13}C NMR ($CDCl_3$): δ 30.2, 47.7, 48.4, 48.5, 119.4, 122.8, 124.1, 124.4, 127.0 and 154.3. Found: C, 71.17; H, 8.11; N, 12.30%. Calcd for $C_{40}H_{50}N_6O_2\cdot1.5H_2O$: C, 71.29; H, 7.93; N, 12.47%. IR (KBr pellets, cm^{-1}): 3409, 3262, 2929, 2825, 1432, 1417, 1185, 845, 777, 749. ESIMS, *m*/*z* 647.1 [M+H]$^+$.

3.6. Synthesis of {H_2[22](DBF)N_2O_3}$\cdot2PF_6$

The compound [22](DBF)N_2O_3 (0.1 g) was dissolved in water/methanol 1:1 (10 cm^{-3}) and HPF_6 (50%) was added until pH 4–5. The solvent was removed under *vacuum*. The solid was dissolved in acetonitrile/ethanol/H_2O (2:2:1). White crystals were formed in few weeks by slow evaporation of the solvent at room temperature.

3.7. Mass spectrometry assays

The compounds were diluted in methanol to a concentration of $1–10\times10^{-6}$ M. Mass spectra for all the compounds have been acquired in the positive polarity mode, after their direct injection into the mass spectrometer using a syringe pump. Mass spectra for compound [17](DBF)N_2O_2 has been acquired at *m*/*z* ranging from 250 to 800 in a LCQ ion trap mass spectrometer equipped with ESI source. The following tune conditions were used: ion spray voltage, 4 kV (positive mode) and temperature of the heated capillary, 250 °C. Nitrogen was used as sheath gas at a flow rate of 20 arbitrary units. Mass spectra for the compounds [22](DBF)N_2O_3, [28](DBF)$_2N_6$ and [32](DBF)$_2N_6$ have been acquired at *m*/*z* ranging from 250 to 1000 in an Esquire ion trap mass spectrometer equipped with ESI source and run by Esquire control. The following tune conditions were used: ion spray voltage, 4 kV (positive mode) and temperature of the heated capillary, 250 °C. Nitrogen was used as drying gas at a flow rate of 5 L/min and at a constant pressure of 15 psi.

3.8. Crystallography

X-ray data for **1** were collected at 150 K on a X-Calibur CCD system. The crystal was positioned at 50 mm from the CCD and 330 frames were measured each for 10 s.

Data for **2** were collected at 298 K on a MAR research Image plate system, respectively. The crystal of **2** was positioned at 70 mm from the image plate. Using an appropriate counting time 95 frames were taken at 2° intervals. Data analysis for **2** was performed with the XDS program.[29] Both data collections were carried out with Mo Kα radiation. The pertinent crystallographic data are given in Table 3.

Table 3. Room temperature crystal data and pertinent refinement details for compounds **1** and **2**

Compound	**1**	**2**
Molecular formula	$\{H_2[22](DBF)N_2O_3\}\cdot 2PF_6$	$[Cu([14](DBF)N_3)(H_2O)_2](SO_4)\cdot 3H_2O$
Empirical formula	$C_{24}H_{34}F_{12}N_2O_4P_2$	$C_{18}H_{31}CuN_3O_{10}S$
M_w	704.47	545.06
Crystal system	Monoclinic	Triclinic
Space group	$P2_1/a$	$P\bar{1}$
a/[Å]	11.4202(10)	9.360(11)
b/[Å]	14.4733(11)	10.223(13)
c/[Å]	18.0700(16)	12.870(15)
α/[°]	(90)	88.64(1)
β/[°]	95.634(7)	68.79(1)
γ/[°]	(90)	80.22(1)
V/[Å^3]	2972.3(4)	1130(2)
Z	4	2
Mg/m^3	1.574	1.601
X-ray system	X-Calibur-CCD	Mar-image plate
μ/[mm^{-1}]	0.256	1.119
Reflections collected	18271	6909
Unique reflections, [R_{int}]	7975[0.0302]	4020[0.0435]
Final R indices		
R_1, wR_2 [$I>2\sigma I$]	0.0421, 0.1040	0.0961, 0.1884
R_1, wR_2 (all data)	0.1015, 0.1101	0.1160, 0.1969
Largest diff. peak and hole	0.317, −0.257	0.521, −0.815

The structures of both compounds were solved by direct methods and by subsequent difference Fourier syntheses and refined by full matrix least squares on F^2 using the SHELX-97 system programs.[30] Anisotropic thermal parameters were used for all non-hydrogen atoms. The hydrogen atoms bonded to carbon and nitrogen atoms were included in refinement at calculated positions while hydrogen atoms of the water molecules were located from difference Fourier maps and refined with O–H distances and H–O–H angles constrained to 0.82 Å and 104.5°, respectively. The thermal movement of hydrogen atoms was described using isotropic parameters equivalent to 1.2 times to that atoms, which were attached. The residual electronic density for both compounds, less than 1 eÅ^{-3}, was within expected values. The molecular diagrams presented were drawn with graphical package software PLATON software package.[31]

Acknowledgements

The authors acknowledge the financial supports from Fundação para a Ciência e a Tecnologia (FCT) and POCTI, with co-participation of the European Community fund FEDER (Project n. POCTI/1999/QUI/35396 and POCTI/QUI/56569/2004). The authors also acknowledge E. Pires (ITQB Mass Spectrometry Analytical Service) for performing the mass spectra acquisition. F.L. acknowledges FCT for the grant (SFRH/BD/9113/2002).

Supplementary data

Supplementary data associated with this article can be found in the online version, at doi:10.1016/j.tet.2006.06.073.

References and notes

1. Llinares, J. M.; Powell, D.; Bowman-James, K. *Coord. Chem. Rev.* **2003**, *240*, 57–75.
2. Ilioudis, C. A.; Steed, J. W. *J. Supramol. Chem.* **2001**, *1*, 165–187.
3. Schmidtchen, F. P.; Berger, M. *Chem. Rev.* **1997**, *97*, 1609–1646.
4. Izatt, R. M.; Pawlak, K.; Bradshaw, J. S. *Chem. Rev.* **1995**, *95*, 2529–2586.
5. Bradshaw, J. S.; Izatt, R. M. *Acc. Chem. Res.* **1997**, *30*, 338–345.
6. Lehn, J. M. *Science (Washington, DC)* **1985**, *227*, 849–856 and references therein.
7. Ashton, P. R.; Chemin, A.; Claessens, C. G.; Menzer, S.; Stoddart, J. F.; White, A. J. P.; Williams, D. J. *Eur. J. Org. Chem.* **1998**, 969–981.
8. Asakawa, M.; Ashton, P. R.; Brown, C. L.; Fyfe, M. C. T.; Menzer, S.; Pasini, D.; Scheuer, C.; Spencer, N.; Stoddart, J. F.; White, A. J. P.; Williams, D. J. *Chem.—Eur. J.* **1997**, *3*, 1136–1150.
9. Schwartz, E. B.; Knobler, C. B.; Cram, D. J. *J. Am. Chem. Soc.* **1992**, *114*, 10775–10784.
10. Helgeson, R. C.; Selle, B. J.; Goldberg, I.; Knobler, C. B.; Cram, D. J. *J. Am. Chem. Soc.* **1993**, *115*, 11506–11511.
11. Agbaria, K.; Biali, S. E. *J. Org. Chem.* **2001**, *66*, 5482–5489.
12. Harmata, M.; Barnes, C. L. *J. Am. Chem. Soc.* **1990**, *112*, 5655–5657.
13. Harmata, M.; Barnes, C. L.; Karra, S. R.; Elahmad, S. *J. Am. Chem. Soc.* **1994**, *116*, 8392–8393.
14. Kanemasa, S.; Oderaotoshi, Y.; Yamamoto, H.; Tanaka, J.; Wada, E. *J. Org. Chem.* **1997**, *62*, 6454–6455.
15. Kanemasa, S.; Oderaotoshi, Y.; Sakaguchi, S.-i.; Yamamoto, H.; Tanaka, J.; Wada, E.; Curran, D. P. *J. Am. Chem. Soc.* **1998**, *120*, 3074–3088.
16. Deng, Y.; Chang, C. J.; Nocera, D. G. *J. Am. Chem. Soc.* **2000**, *122*, 410–411.
17. Lashuel, H. A.; LaBrenz, S. R.; Woo, L.; Serpell, L. C.; Kelly, J. W. *J. Am. Chem. Soc.* **2000**, *122*, 5262–5277.
18. Kaul, R.; Deechongkit, S.; Kelly, J. W. *J. Am. Chem. Soc.* **2002**, *124*, 11900–11907.
19. Deechongkit, S.; Powers, E. T.; You, S.-L.; Kelly, J. W. *J. Am. Chem. Soc.* **2005**, *127*, 8562–8570.
20. Vigato, P. A.; Tamburini, S. *Coord. Chem. Rev.* **2004**, *248*, 1717–2128.

21. Vance, A. L.; Alcock, N. W.; Busch, D. H.; Heppert, J. A. *Inorg. Chem.* **1997**, *36*, 5132–5134.
22. Chen, D.; Martell, A. E. *Tetrahedron* **1991**, *47*, 6895–6902.
23. Li, F.; Delgado, R.; Costa, J.; Drew, M. G. B.; Félix, V. *Dalton Trans.* **2005**, 82–91 and references therein.
24. (a) Allen, F. H. *Acta Crystallogr.* **2002**, *B58*, 380–388; (b) Bruno, I. J.; Cole, J. C.; Edginton, P. R.; Kessler, M.; Macrae, C. F.; McCabe, P.; Pearson, J.; Taylor, R. *Acta Crystallogr.* **2002**, *B58*, 389–397.
25. Case, D. A.; Darden, T. A.; Cheatham, T. E., III; Simmerling, C. L.; Wang, J.; Duke, R. E.; Luo, R.; Merez, K. M.; Wang, B.; Pearlman, D. A.; Crowley, M.; Brozell, S.; Tsui, V.; Gohlke, H.; Mongan, J.; Hornak, V.; Cui, G.; Beroza, P.; Schafmeister, C.; Caldwell, J. W.; Ross, W. S.; Kollman, P. A. *AMBER Version 8*; University of California: San Francisco, CA, 2004.
26. GAFF force field; Wang, J.; Wolf, R. M.; Caldwell, J. W.; Kollmann, P. A.; Case, D. A. *J. Comput. Chem.* **2004**, *25*, 1157–1174.
27. Jakalian, A.; Bush, B. L.; Jack, D. B.; Bayly, C. I. *J. Comput. Chem.* **2000**, *21*, 132–146.
28. Skar, M. L.; Svendsen, J. S. *Tetrahedron* **1997**, *53*, 17425–17440.
29. Kabsch, W. *J. Appl. Crystallogr.* **1988**, *21*, 916–924.
30. Sheldrick, G. M. *SHELX-97*; University of Göttingen: Göttingen, Germany, 1997.
31. Spek, L. *PLATON, A Multipurpose Crystallographic Tool*; Utrecht University: Utrecht, The Netherlands, 1999.